Letter

μ^+ Knight shift in UTe_2: Evidence for relocalization in a Kondo lattice

N. Azari,[1] M. R. Goeks,[1] M. Yakovlev,[1] M. Abedi,[1] S. R. Dunsiger,[1,2] S. M. Thomas,[3] J. D. Thompson,[3] P. F. S. Rosa,[3] and J. E. Sonier[1]

[1]*Department of Physics, Simon Fraser University, Burnaby, British Columbia, Canada V5A 1S6*
[2]*Centre for Molecular and Materials Science, TRIUMF, Vancouver, British Columbia, Canada V6T 2A3*
[3]*Los Alamos National Laboratory, Los Alamos, New Mexico 87545, USA*

(Received 21 April 2023; revised 19 June 2023; accepted 14 July 2023; published 4 August 2023)

The local magnetic susceptibility of the spin-triplet superconductor UTe_2 has been investigated by positive muon (μ^+) Knight shift measurements in the normal state. Three distinct μ^+ Knight shift components are observed for a magnetic field applied parallel to the c axis. Two of these exhibit a breakdown in the linear relationship with the bulk magnetic susceptibility (χ) below a temperature $T^* \sim 30$ K, which points to a gradual emergence of a correlated Kondo liquid. Below $T_r \sim 12$ K linearity is gradually restored, indicating relocalization of the Kondo liquid quasiparticles. The third Knight shift component is two orders of magnitude larger, and despite the c-axis alignment of the external field, scales with the a axis χ above $T_r \sim 12$ K. We conjecture that this component is associated with magnetic clusters and the change in the temperature dependence of all three Knight shift components below T_r is associated with a change in magnetic correlations. Our findings indicate that prior to the onset of superconductivity the development of the itinerant heavy-electron fluid is halted by a gradual development of local U $5f$-moment fluctuations.

DOI: 10.1103/PhysRevB.108.L081103

Solid-state materials exhibiting odd-parity superconductivity have long been of fundamental interest. Today these are recognized as holding great promise for providing practical solutions to limitations in spintronics [1,2] and quantum computing technologies [3,4]. The heavy-fermion compound UTe_2 has emerged as a potential solid-state spin-triplet superconductor [5]. Evidence for UTe_2 being an odd-parity superconductor includes a minor change in the ^{125}Te nuclear magnetic resonance (NMR) Knight shift below the superconducting critical temperature (T_c) [5,6], a large anisotropic upper critical field (H_{c2}) that greatly exceeds the Pauli paramagnetic limit [5,7], and reentrant superconductivity for magnetic fields greatly exceeding H_{c2} applied in certain crystallographic directions [8,9]. Further characteristics of the superconducting pairing state in UTe_2 deduced by experiments include evidence for chiral surface states [10] and a two-component superconducting order parameter that breaks time-reversal symmetry [11].

Within conventional spin-fluctuation theory, odd-parity pairing is expected to be mediated by ferromagnetic (FM) fluctuations [12]. Shortly after the discovery of superconductivity in UTe_2, evidence for low-temperature FM spin fluctuations was found by muon spin rotation/relaxation (μSR) [13] and NMR [14] studies. Yet only antiferromagnetic (AFM) spin fluctuations have been detected in subsequent inelastic neutron scattering (INS) experiments [15,16], which also observe a spin resonance near an incommensurate AFM wave vector below T_c [17,18]. Furthermore, applied hydrostatic pressure above 1.3 GPa appears to induce an AFM phase [19]. These findings have motivated the development of theoretical models for spin-triplet pairing driven by AFM spin fluctuations [20–22] and highlighted the possibility of coexisting FM and AFM spin fluctuations [23]. A picture in which FM coupling is dominant within the U-ladder structure of UTe_2, while AFM coupling is dominant between the ladders, has been proposed in neutron [16] and NMR [24] studies.

Experimental observations indicate that the superconducting state of UTe_2 emerges from a well-developed heavy Fermi liquid. In particular, the temperature dependence of the electronic specific heat ($C_{el} \propto T$) and the electrical resistivity ($\rho \propto T^2$) below $T \sim 5$ K [5], and a nearly constant value of the normal-state ^{125}Te-NMR spin-lattice relaxation rate divided by temperature ($1/T_1T$) below 10–15 K for external magnetic fields $\mathbf{H} \parallel \mathbf{b}$ and $\mathbf{H} \parallel \mathbf{c}$ [14,24,25], are typical Fermi-liquid behavior. Recently, it has been proposed that spin-triplet superconductivity in UTe_2 can arise from the delocalization of preformed Hund's coupling induced spin-triplet pairs by coherent Kondo hybridization [26]. But at present, the nature of the interactions responsible for superconductivity in UTe_2 is unresolved.

Here, we report on the utilization of μSR to probe the local magnetic susceptibility of a UTe_2 single crystal grown by a chemical vapor transport (CVT) method [27]. Our results demonstrate a significant relocalizaton of the $5f$ electrons prior to the onset of superconductivity. Specific heat measurements show the crystal to be superconducting below $T_c = 1.90(5)$ K with a residual T-linear term coefficient $\gamma^* = 41(1)$ mJ/mol K^2. Figure 1 shows a comparison of the temperature dependence of the normal-state bulk magnetic susceptibility (χ) for a magnetic field of 1 kOe applied parallel to the three principal crystallographic axes, herein denoted χ_a, χ_b, and χ_c. A plot of χ_c^{-1} vs T for $\mathbf{H} \parallel \mathbf{c}$ exhibits a linear dependence between 150 and 350 K (see Fig. S1 [28]). A fit over this range to a Curie-Weiss law yields a Curie-Weiss temperature $\Theta = -128.0(4)$ K and an effective

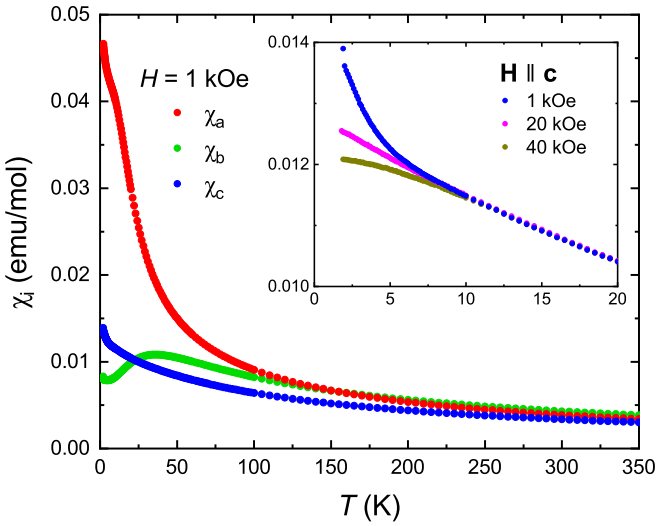

FIG. 1. Temperature dependence of the bulk magnetic susceptibility of the UTe_2 sample for a magnetic field $H = 1$ kOe applied parallel to the three different principal crystallographic axes. The inset shows the low-temperature behavior of $\chi_c(T)$ for different values of the magnetic field applied parallel to the c axis.

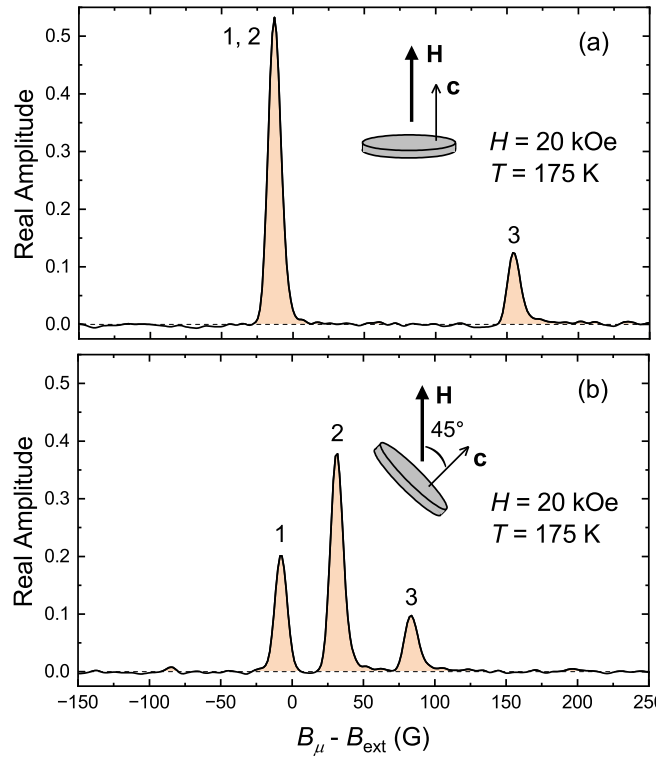

FIG. 2. Fourier transform of the TF-μSR asymmetry spectrum for the UTe_2 single crystal at $T = 175$ K in a magnetic field $H = 20$ kOe applied (a) parallel to the c axis, and (b) at an angle of 45° with respect to the c axis. Note, for (b) the orientation of the component of **H** in the a-b plane is unknown.

moment of $3.39(8)\mu_B$/U calculated from the Curie constant, which are in good agreement with previously reported $\chi_c(T)$ data [5,7,27,29]. The inset of Fig. 1 shows that $\chi_c(T)$ develops a field dependence below $T \sim 10$ K, which is also the case for $\chi_a(T)$.

Our μSR measurements were performed using the NuTime spectrometer at the TRIUMF Centre for Molecular and Materials Science. Most of the measurements were done with **H** applied parallel to the c axis (**H** ∥ **c**) and perpendicular to the initial muon spin polarization $\mathbf{P}_\mu(0)$, in a so-called transverse field (TF) configuration. The muon spin precesses about the local magnetic field $\mathbf{B}_\mu$ at its stopping site with a frequency $f_\mu = \gamma_\mu B_\mu/2\pi$, where $\gamma_\mu/(2\pi) = 135.54$ MHz/T is the muon gyromagnetic ratio. The frequency f_μ is obtained from the oscillatory TF-μSR asymmetry spectrum (see Fig. S2 [28]), which follows the time evolution of the muon spin polarization $\mathbf{P}_\mu(t)$ of the implanted μ^+ ensemble. The local field $\mathbf{B}_\mu$ in UTe_2 is the vector sum of **H**, demagnetization, and Lorentz fields, and the polarization of the conduction electrons and localized U $5f$-electron moments induced by the applied field [30]. The relative field shift $K^* = (B_\mu - H)/H$ at each temperature was accurately determined using a custom sample holder [31], where H is obtained from μ^+ stopping in a pure Ag mask upstream from the sample. A separate background-free TF-μSR signal was generated by μ^+ passing through the 3-mm-diameter hole in the Ag mask and subsequently stopping in the UTe_2 single crystal. Correcting K^* for the demagnetization and Lorentz fields yields the μ^+ Knight shift

$$K = K_0 + K_{5f}. \tag{1}$$

The term K_0 is due to the Pauli paramagnetism of the conduction electrons sensed by the μ^+ via the Fermi contact interaction. The second term K_{5f} is proportional to the susceptibility of the localized U $5f$ moments $\chi_{5f}(T)$, which has two contributions: (i) the direct dipole-dipole interaction between the local $5f$ moments and the μ^+, and (ii) the additional polarization of the conduction electrons by the Ruderman-Kittel-Kasuya-Yosida (RKKY) interaction with the localized moments. The formation of a heavy-electron fluid introduces an additional local magnetic susceptibility component $\chi_{HF}(T)$ that the μ^+ may couple to.

Figure 2(a) shows a Fourier transform of the TF-μSR signal in UTe_2 at $T = 175$ K for **H** ∥ **c**. Two distinct peaks are observed. The smaller peak on the far right originates from ∼18% of the sample and exhibits a substantial relative field shift as the temperature is lowered (see Fig. S3 [28]). The larger peak originating from the rest of the sample actually consists of two closely spaced peaks, but these are not visually evident due to the broadening effects of the apodization function used to generate the Fourier transform. As shown in Fig. 2(b), a clear splitting of the larger peak occurs for **H** rotated at an angle of 45° with respect to the c axis. Indeed, we find the TF-μSR asymmetry spectrum for **H** ∥ **c** is best described by the sum of three (rather than two) oscillating components as follows,

$$A(t) = a_0 P_\mu(t) = \sum_{i=1}^{3} a_i e^{-\sigma_i t^2} \cos(\gamma_\mu B_i t/2\pi + \phi_i), \tag{2}$$

where a_0 is the total initial asymmetry and a_i, σ_i, B_i, and ϕ_i are the initial asymmetry, depolarization rate, average

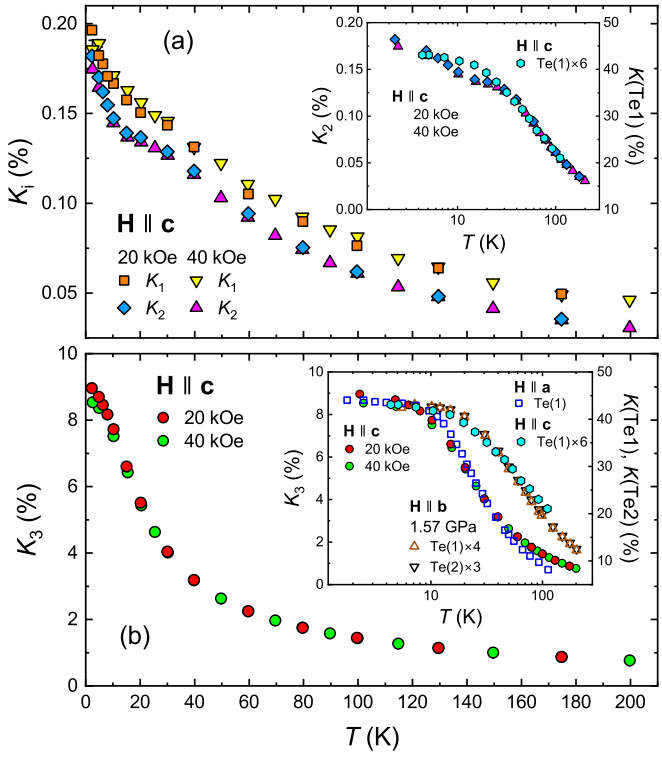

FIG. 3. Temperature dependence of the μ^+ Knight shifts (a) K_i ($i = 1$, 2) and (b) K_3 for magnetic fields $H = 20$ kOe and $H =$ 40 kOe applied parallel to the c axis. The insets in (a) and (b) show a comparison of $K_2(T)$ and $K_3(T)$ to the temperature dependence of the ^{125}Te NMR Knight shift at the Te(1) site in UTe_2 for **H** ∥ **c** [14]. The inset of (b) also shows the temperature dependence of the ^{125}Te NMR Knight shift at the Te(1) site for **H** ∥ **a** [33] and at the Te(1) and Te(2) sites for **H** ∥ **b** and an applied pressure of 1.57 GPa [24]. Note, for comparison the NMR Knight shift data for **H** ∥ **a** and **H** ∥ **c** have been multiplied by different scaling factors.

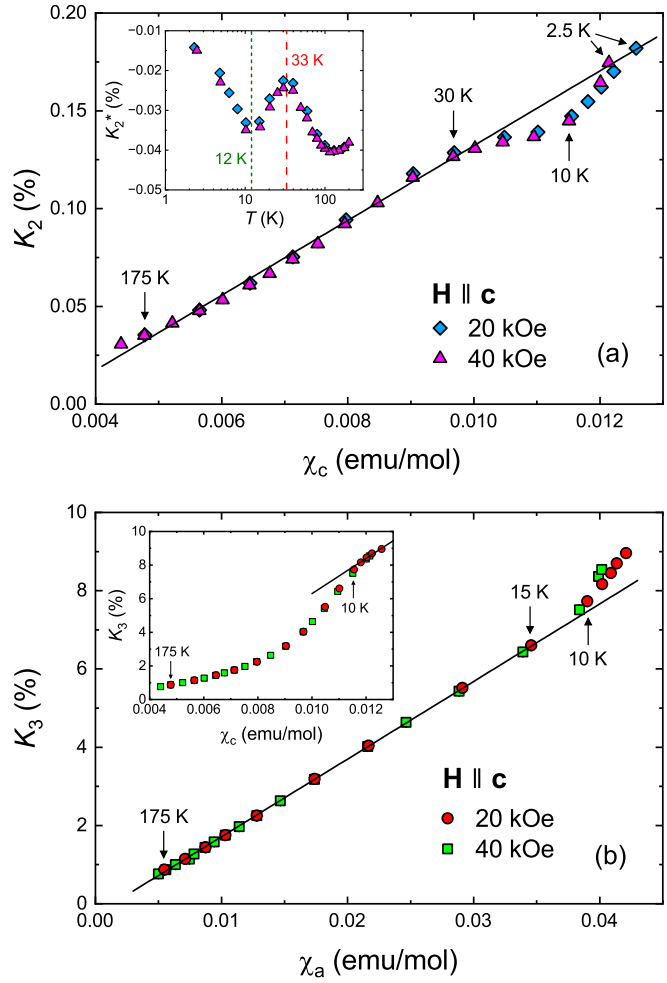

FIG. 4. (a) Plot of K_2 vs the bulk magnetic susceptibility for **H** ∥ **c**. The inset shows the temperature dependence of the relative field shift K_2^*. (b) Plot of K_3 for **H** ∥ **c** vs the bulk magnetic susceptibility for **H** ∥ **a**. The inset shows K_3 vs the bulk magnetic susceptibility for **H** ∥ **c**. The straight line through the data in the main panels and the inset in (b) are linear fits described in the main text.

internal field, and phase angle of the individual components. Fits to Eq. (2) yield the temperature-independent values $a_1 =$ 27(2)%, $a_2 = 55(2)$%, and $a_3 = 18.2(1)$% (see Fig. S2 [28]), which are a measure of magnetic sample volume fractions.

Figure 3 shows the temperature dependence of the normal-state μ^+ Knight shifts for **H** ∥ **c** associated with each of the three oscillating components in Eq. (2). Since density functional theory (DFT) calculations predict a single crystallographic μ^+ site in UTe_2 [32], the similar behavior of $K_1(T)$ and $K_2(T)$ suggests these components are associated with two magnetically inequivalent μ^+ sites. The inset of Fig. 3(a) shows that $K_2(T)$ tracks the Te(1)-site NMR Knight shift for **H** ∥ **c** [14] down to ∼30 K. By contrast, the large μ^+ Knight shift $K_3(T)$ instead more closely follows the Te(1)-site NMR Knight shift for **H** ∥ **a** [33], as shown in the inset of Fig. 3(b).

Figure 4(a) shows a plot of K_2 versus the bulk magnetic susceptibility χ_c with temperature as an implicit parameter. Both K_2 and K_1 (see Fig. S4 [28]) exhibit a linear dependence on χ_c down to $T \sim 30$ K, below which the local magnetic susceptibility sensed by the μ^+ deviates from χ_c. A fit of the K_2 vs χ_c data over the temperature range 30–200 K to $K_2 = A\chi_c/0.55 + K_0$ yields $A = 587(12)$ Oe/μ_B and $K_0 = -590(27)$ ppm. Below $T \sim 30$ K, K_2 and K_1 vs χ_c deviate from linearity. In heavy-fermion materials with concentrated f moments, a low-temperature Knight shift anomaly marked by $K(T)$ deviating from a linear relation with $\chi(T)$ typically signifies the onset of coherent Kondo screening of the local f moments [34]. In UTe_2, the development of Kondo coherence manifests as a rapid drop in the a-axis and b-axis resistivities below ∼50 K [35] and a Fano-shaped resonance in the differential conductance measured by scanning tunneling microscopy [10]. The Kondo coherence temperature has been estimated to be $T^* = 20$–26 K from fits of the Fano resonance. Although broad maxima in the temperature dependences of χ_b and the ^{125}Te NMR Knight shift for **H** ∥ **b** near 35–40 K [14,24,29] may be interpreted as the development of AFM correlations and the formation of Kondo coherence, this feature can be also explained by crystal electric field (CEF) effects [27]. Surprisingly, only a subtle ^{125}Te-NMR Knight shift anomaly has been identified in UTe_2 below $T \sim 30$ K at the Te(1) site for **H** ∥ **b** [24].

Based on a two-fluid description of the Kondo lattice [36], whereby collective hybridization between localized f and conduction electrons leads to the formation of an itinerant heavy-fermion fluid coexisting with a lattice of partially screened local f moments, the NMR Knight shift is described by [34]

$$K(T) = A\chi_{cc}(T) + (A+B)\chi_{cf}(T) + B\chi_{ff}(T), \quad (3)$$

where χ_{cc}, χ_{ff}, and χ_{cf} are spin susceptibilities associated with the unhybridized conduction electrons, unhybridized local f moments, and spin polarization of the conduction electrons by the correlated f moments, A is a coupling constant associated with the on-site hyperfine interaction of the nuclear spin with the conduction electrons, and B is a coupling constant associated with a transferred hyperfine interaction via orbital overlap with the localized f wave function on neighboring atoms and an indirect interaction with the local f moments mediated by the conduction electrons. In the two-fluid model $\chi(T) = \chi_{cc}(T) + 2\chi_{cf}(T) + \chi_{ff}(T)$. An NMR Knight shift anomaly generally occurs with the emergence of the itinerant heavy-fermion fluid due to $\chi_{cf}(T)$ and $\chi_{ff}(T)$ having different temperature dependences, unless $A = B$, in which case $K(T) \propto \chi(T)$. The weakness or absence of a ^{125}Te-NMR Knight shift anomaly in UTe_2 may be due to A and B being very close in value, as found to be the case for certain nuclei and external field directions in other heavy-fermion compounds [34,37]. The clear Knight shift anomaly observed by μSR could be due to a difference in sample quality or may be a consequence of the different way the μ^+ senses the local $5f$ moments, as described below Eq. (1).

At temperatures above T^*, $\chi_c(T)$ is dominated by the unhybridized local $5f$ moments, so that $K_2 \propto \chi_c \approx \chi_{ff}$. The deviation from this linear relation that occurs below $\sim$30 K diminishes below $T_r \sim 12$ K, and linear scaling appears to be restored at $T \sim 2.5$ K [see Fig. 4(a)]. This suggests there is a transfer of the $5f$-electron spectral weight from the itinerant heavy-electron fluid back to the partially screened local moments, as has been observed in NMR Knight shift measurements on $CePt_2In_7$ [38] and $CeRhIn_5$ [39]. In the latter heavy-fermion materials this reverse transfer (relocalization) is partial and is a consequence of developing AFM correlations between partially screened local $4f$ moments that are a precursor to long-range magnetic order at lower temperature. In UTe_2 superconductivity preempts a magnetically ordered state of the relocalized moments.

As shown in Fig. 4(b), despite the $\mathbf{H} \parallel \mathbf{c}$ alignment K_3 exhibits the unusual linear relationship $K_3 \propto \chi_a$ above $\sim$10 K. A fit of the K_3 vs χ_a data over the temperature range 15–200 K to $K_3 = A\chi_a/0.18 + K_0$ yields $A = 1994(6)$ Oe/μ_B and $K_0 = -2.7(1) \times 10^3$ ppm. The large value of K_0 is unphysical if due solely to the Pauli paramagnetism of the conduction electrons, while the high value of K_3 suggests this component is associated with unhybridized local $5f$ moments and a large effective moment. We conjecture that K_3 is due to the presence of magnetic clusters, which we have recently argued to be the source of the ubiquitous residual T-linear term in the specific heat $C(T)$ and upturn in C/T vs T at low temperatures [32]. The magnetic cluster volume fraction deduced from weak TF-μSR measurements was observed to be larger in a UTe_2 sample with a higher residual T-linear term coefficient γ^*. The value of γ^* for the current sample is consistent with this previous study if the 18% of the sample associated with K_3 is due to magnetic clusters.

The depolarization rate σ_3 associated with K_3 increases rapidly below 20 K (see Fig. S5 [28]) and reaches a value at 2.5 K corresponding to an internal field distribution of rms width $\Delta B_{\rm rms} = \sigma_3/\gamma_\mu = 45$ and 57 G for $H = 20$ and 40 kOe, respectively. Consequently, while the component K_3 may manifest as a high-frequency peak in the NMR line shape, it may be wiped out by a large spread in resonance frequencies. The origin of the magnetic clusters remains unknown, although it has been suggested that they are the result of local disorder/defect induced disruptions of long-range FM correlations within the U-ladder sublattice structure [33]. The observed scaling $K_3 \propto \chi_a$ for $\mathbf{H} \parallel \mathbf{c}$ suggests that the effective moment of the magnetic clusters is essentially locked along the a axis above $\sim$10 K, but at lower temperatures appears free to rotate resulting in the $K_3 \propto \chi_c$ behavior shown in the inset of Fig. 4(b). Presumably this change is triggered by the same source responsible for relocalization in a majority (82%) of the sample.

The onset of gradual relocalization at $T_r \sim 12$ K basically coincides with the strong increase of $\chi_a(T)$ with decreasing temperature, a saturation of the real part of the static susceptibility in INS measurements [16], a broad minimum in the electronic contribution to the c-axis thermal expansion, and broad peaks in the temperature derivative of the a-axis resistivity and the electronic contribution to the specific heat $C_{\rm el}/T$ [40,41]. The maximum in $C_{\rm el}/T$ at 12–14 K has recently been attributed to CEF splitting of the ground state degenerate J multiplet of U^{4+} ($5f^2$ electron configuration) into singlet states [42]. A similar CEF splitting of the U-$5f^2$ ground state multiplet has been previously proposed to prompt partial arrest of a two-channel Kondo effect in URu_2Si_2 at temperatures below the energy splitting of the two lowest-lying singlets, resulting in a transition to "hidden multipolar order" and a pressure-induced large-moment AFM phase [43]. While there is a pressure-induced AFM phase in UTe_2 [19], there is no long-range multipolar or magnetic order in UTe_2 at ambient pressure [13,44]. This could be because the different singlets do not have the right symmetries to generate multipolar degrees of freedom or that the exchange interactions between the U-$5f^2$ ions are relatively weak compared to the CEF splitting—perhaps sufficient though to induce critical fluctuations of orbital magnetic dipole and multipole degrees of freedom that could mediate superconducting pairing [42].

Our findings suggest that the evolution of the heavy-electron Fermi liquid in UTe_2 is halted by the development of critical localized spin fluctuations below $T_r \sim 12$ K. While the cause is not known with certainty, this also appears to unlock the magnetic moment of defect-induced magnetic clusters from the a axis. Remarkably, the relocalization of the U-$5f$ moments does not influence signatures of the heavy-electron Fermi liquid in transport and NMR $1/T_1T$ measurements. The coexistence of decoupled localized moments and a Fermi

liquid in UTe_2 may be a consequence of an underscreened Kondo lattice [45]. Although electron pairing in the superconducting phase of UTe_2 may be mediated by either spin fluctuations associated with itinerant-electron interactions or magnetic interactions of localized moments, the pairing may instead arise from a coupling of the itinerant electrons to the local moments.

We thank N. J. Curro and J. Paglione for informative discussions. J.E.S. and S.R.D. acknowledge support from the Natural Sciences and Engineering Research Council of Canada (PIN 146772). Work at Los Alamos National Laboratory by S.M.T., J.D.T., and P.F.S.R. was supported by the U.S. Department of Energy, and the Office of Basic Energy Sciences, Division of Materials Science.

[1] M. Eschrig, Spin-polarized supercurrents for spintronics: a review of current progress, Rep. Prog. Phys. **78**, 104501 (2015).

[2] J. Linder and J. W. A. Robinson, Superconducting spintronics, Nat. Phys. **11**, 307 (2015).

[3] A. M. Gulian and K. S. Wood, Triplet superconductors from the viewpoint of basic elements for quantum computers, IEEE Trans. Appl. Supercond. **13**, 944 (2003).

[4] E. Gibney, Inside Microsoft's quest for a topological quantum computer, Nature (London) (2016), doi:10.1038/nature.2016.20774.

[5] S. Ran, C. Eckberg, Q.-P. Ding, Y. Furukawa, T. Metz, S. R. Saha, I.-L. Liu, M. Zic, H. Kim, J. Paglione, and N. P. Butch, Newly ferromagnetic spin-triplet superconductivity, Science **365**, 684 (2019).

[6] G. Nakamine, S. Kitagawa, K. Ishida, Y. Tokunaga, H. Sakai, S. Kambe, A. Nakamura, Y. Shimizu, Y. Homma, D. Li, F. Honda, and D. Aoki, Superconducting properties of heavy fermion UTe_2 revealed by ^{125}Te-nuclear magnetic resonance, J. Phys. Soc. Jpn. **88**, 113703 (2019).

[7] D. Aoki, A. Nakamura, F. Honda, D. Li, Y. Homma, Y. Shimizu, Y. J. Sato, G. Knebel, J.-P. Brison, A. Pourret, D. Braithwaite, G. Lapertot, Q. Niu, M. Vališka, H. Harima, and J. Flouquet, Unconventional superconductivity in heavy fermion UTe_2, J. Phys. Soc. Jpn. **88**, 043702 (2019).

[8] S. Ran, I.-L. Liu, Y. S. Eo, D. J. Campbell, P. M. Neves, W. T. Fuhrman, S. R. Saha, C. Eckberg, H. Kim, D. Graf, F. Balakirev, J. Singleton, J. Paglione, and N. P. Butch, Extreme magnetic field-boosted superconductivity, Nat. Phys. **15**, 1250 (2019).

[9] G. Knebel, W. Knafo, A. Pourret, Q. Niu, M. Vališka, D. Braithwaite, G. Lapertot, M. Nardone, A. Zitouni, S. Mishra, I. Sheikin, G. Seyfarth, J.-P. Brison, D. Aoki, and J. Flouquet, Field-reentrant superconductivity close to a metamagnetic transition in the heavy-fermion superconductor UTe_2, J. Phys. Soc. Jpn. **88**, 063707 (2019).

[10] L. Jiao, S. Howard, S. Ran, Z. Wang, J. O. Rodriguez, M. Sigrist, Z. Wang, N. P. Butch, and V. Madhavan, Chiral superconductivity in heavy-fermion metal UTe_2, Nature (London) **579**, 523 (2020).

[11] I. M. Hayes, D. S. Wei, T. Metz, J. Zhang, Y. S. Eo, S. Ran, S. R. Saha, J. Collini, N. P. Butch, D. F. Agterberg, A. Kapitulnik, and J. Paglione, Multicomponent superconducting order parameter in UTe_2, Science **373**, 797 (2021).

[12] M. Sigrist, Introduction to unconventional superconductivity, AIP Conf. Proc. **789**, 165 (2005).

[13] S. Sundar, S. Gheidi, K. Akintola, A. M. Côté, S. R. Dunsiger, S. Ran, N. P. Butch, S. R. Saha, J. Paglione, and J. E. Sonier, Coexistence of ferromagnetic fluctuations and superconductivity in the actinide superconductor UTe_2, Phys. Rev. B **100**, 140502(R) (2019).

[14] Y. Tokunaga, H. Sakai, S. Kambe, T. Hattori, N. Higa, G. Nakamine, S. Kitagawa, K. Ishida, A. Nakamura, Y. Shimizu, Y. Homma, D. Li, F. Honda, and D. Aoki, ^{125}Te NMR study on a single crystal of heavy fermion superconductor UTe_2, J. Phys. Soc. Jpn. **88**, 073701 (2019).

[15] C. Duan, K. Sasmal, M. B. Maple, A. Podlesnyak, J.-X. Zhu, Q. Si, and P. Dai, Incommensurate Spin Fluctuations in the Spin-Triplet Superconductor Candidate UTe_2, Phys. Rev. Lett. **125**, 237003 (2020).

[16] W. Knafo, G. Knebel, P. Steffens, K. Kaneko, A. Rosuel, J.-P. Brison, J. Flouquet, D. Aoki, G. Lapertot, and S. Raymond, Low-dimensional antiferromagnetic fluctuations in the heavy-fermion paramagnetic ladder compound UTe_2, Phys. Rev. B **104**, L100409 (2021).

[17] C. Duan, R. E. Baumbach, A. Podlesnyak, Y. Deng, C. Moir, A. J. Breindel, M. B. Maple, E. M. Nica, Q. Si, and P. Dai, Resonance from antiferromagnetic spin fluctuations for superconductivity in UTe_2, Nature (London) **600**, 636 (2021).

[18] S. Raymond, W. Knafo, G. Knebel, K. Kaneko, J.-P. Brison, J. Flouquet, D. Aoki, and G. Lapertot, Feedback of superconductivity on the magnetic excitation spectrum of UTe_2, J. Phys. Soc. Jpn. **90**, 113706 (2021).

[19] S. M. Thomas, F. B. Santos, M. H. Christensen, T. Asaba, F. Ronning, J. D. Thompson, E. D. Bauer, R. M. Fernandes, G. Fabbris, and P. F. S. Rosa, Evidence for a pressure-induced antiferromagnetic quantum critical point in intermediate-valence UTe_2, Sci. Adv. **6**, eabc8709 (2020).

[20] A. Kreisel, Y. Quan, and P. Hirschfeld, Spin-triplet superconductivity driven by finite-momentum spin fluctuations, Phys. Rev. B **105**, 104507 (2022).

[21] L. Chen, H. Hu. C. Lane, E. M. Nica, J.-X. Zhu, and Q. Si, Multiorbital spin-triplet pairing and spin resonance in the heavy-fermion superconductor UTe_2, arXiv:2112.14750.

[22] D. Shaffer and D. V. Chichinadze, Chiral superconductivity in UTe_2 via emergent C_4 symmetry and spin-orbit coupling, Phys. Rev. B **106**, 014502 (2022).

[23] Y. Xu, Y. Sheng, and Y.-f. Yang, Quasi-Two-Dimensional Fermi Surfaces and Unitary Spin-Triplet Pairing in the Heavy Fermion Superconductor UTe_2, Phys. Rev. Lett. **123**, 217002 (2019).

[24] D. V. Ambika, Q.-P. Ding, K. Rana, C. E. Frank, E. L. Green, S. Ran, N. P. Butch, and Y. Furukawa, Possible coexistence of antiferromagnetic and ferromagnetic spin fluctuations in the spin-triplet superconductor UTe_2 revealed by ^{125}Te NMR under pressure, Phys. Rev. B **105**, L220403 (2022).

[25] K. Kinjo, H. Fujibayashi, G. Nakamine, S. Kitagawa, K. Ishida, Y. Tokunaga, H. Sakai, S. Kambe, A. Nakamura, Y. Shimizu, Y. Homma, D. Li, F. Honda, and D. Aoki, Drastic change in

magnetic anisotropy of UTe_2 under pressure revealed by ^{125}Te-NMR, Phys. Rev. B **105**, L140502 (2022).

[26] T. Hazra and P. Coleman, Triplet Pairing Mechanisms from Hund's-Kondo Models: Applications to UTe_2 and $CeRh_2As_2$, Phys. Rev. Lett. **130**, 136002 (2023).

[27] P. F. S. Rosa, A. Weiland, S. S. Fender, B. L. Scott, F. Ronning, J. D. Thompson, E. D. Bauer, and S. M. Thomas, Single thermodynamic transition at 2 K in superconducting UTe_2 single crystals at 2 K, Commun. Mater. **3**, 33 (2022).

[28] See Supplemental Material at http://link.aps.org/supplemental/10.1103/PhysRevB.108.L081103 for a fit of the χ_c data to a Curie-Weiss law; representative TF-μSR asymmetry spectrum and Fourier transforms of TF-μSR asymmetry spectra showing how the different contributions to the signal change with temperature; plot of the μ^+-Knight shift component K_1 vs χ_c with temperature as an implicit parameter; and the temperature dependence of the fitted values of the Gaussian relaxation rates σ_1, σ_2, and σ_3.

[29] S. Ikeda, H. Sakai, D. Aoki, Y. Homma, E. Yamamoto, A. Nakamura, Y. Shiokawa, Y. Haga, and Y. Ōnuki, Single crystal growth and magnetic properties of UTe_2, J. Phys. Soc. Jpn. Suppl. **75**, 116 (2006).

[30] A. Amato, Heavy-fermion systems studied by μSR technique, Rev. Mod. Phys. **69**, 1119 (1997).

[31] K. Akintola, A. Pal, S. R. Dunsiger, A. C. Y. Fang, M. Potma, S. R. Saha, X. Wang, J. Paglione, and J. E. Sonier, Freezing out of a low-energy bulk spin exciton in SmB_6, npj Quantum Mater. **3**, 36 (2018).

[32] S. Sundar, N. Azari, M. R. Goeks, S. Gheidi, M. Abedi, M. Yakovlev, S. R. Dunsiger, J. M. Wilkinson, S. J. Blundell, T. E. Metz, I. M. Hayes, S. R. Saha, S. Lee, A. J. Woods, R. Movshovich, S. M. Thomas, N. P. Butch, P. F. S. Rosa, J. Paglione, and J. E. Sonier, Ubiquitous spin freezing in the superconducting state of UTe_2, Commun. Phys. **6**, 24 (2023).

[33] Y. Tokunaga, H. Sakai, S. Kambe, Y. Haga, Y. Tokiwa, P. Opletal, H. Fujibayashi, K. Kinjo, S. Kitagawa, K. Ishida, A. Nakamura, Y. Shimizu, Y. Homma, D. Li, F. Honda, and D. Aoki, Slow electronic dynamics in the paramagnetic state of UTe_2, J. Phys. Soc. Jpn. **91**, 023707 (2022).

[34] N. J. Curro, B.-L. Young, J. Schmalian, and D. Pines, Scaling in the emergent behavior of heavy-electron materials, Phys. Rev. B **70**, 235117 (2004).

[35] Y. S. Eo, S. Liu, S. R. Saha, H. Kim, S. Ran, J. A. Horn, H. Hodovanets, J. Collini, T. Metz, W. T. Fuhrman, A. H. Nevidomskyy, J. D. Denlinger, N. P. Butch, M. S. Fuhrer, L. A. Wray, and J. Paglione, c-axis transport in UTe_2: Evidence of three-dimensional conductivity component, Phys. Rev. B **106**, L060505 (2022).

[36] S. Nakatsuji, D. Pines, and Z. Fisk, Two Fluid Description of the Kondo Lattice, Phys. Rev. Lett. **92**, 016401 (2004).

[37] N. J. Curro, B. Simovic, P. C. Hammel, P. G. Pagliuso, J. L. Sarrao, J. D. Thompson, and G. B. Martins, Anomalous NMR magnetic shifts in $CeCoIn_5$, Phys. Rev. B **64**, 180514(R) (2001).

[38] N. apRoberts-Warren, A. P. Dioguardi, A. C. Shockley, C. H. Lin, J. Crocker, P. Klavins, D. Pines, Y.-F. Yang, and N. J. Curro, Kondo liquid emergence and relocalization in the approach to antiferromagnetic ordering in $CePt_2In_7$, Phys. Rev. B **83**, 060408(R) (2011).

[39] K. R. Shirer, A. C. Shockley, A. P. Dioguardi, J. Crocker, C. H. Lin, N. apRoberts-Warren, D. M. Nisson, P. Klavins, J. C. Cooley, Y.-F. Yang, and N. J. Curro, Long range order and two-fluid behavior in heavy electron materials, Proc. Natl. Acad. Sci. USA **109**, E3067 (2012).

[40] K. Willa, F. Hardy, D. Aoki, D. Li, P. Wiecki, G. Lapertot, and C. Meingast, Thermodynamic signatures of short-range magnetic correlations in UTe_2, Phys. Rev. B **104**, 205107 (2021).

[41] Y. Haga, P. Opletal, Y. Tokiwa, E. Yamamoto, Y. Tokunaga, S. Kambe, and H Sakai, Effect of uranium deficiency on normal and superconducting properties in unconventional superconductor UTe_2, J. Phys.: Condens. Matter **34**, 175601 (2022).

[42] S. Khmelevskyi, L. V. Pourovskii, and E. A. Tereshina-Chitrova, Structure of the normal state and origin of Schottky anomaly in the correlated heavy fermion superconductor UTe_2, Phys. Rev. B **107**, 214501 (2023).

[43] K. Haule and G. Kotliar, Arrested Kondo effect and hidden order in URu_2Si_2, Nat. Phys. **5**, 796 (2009).

[44] V. Hutanu, H. Deng, S. Ran, W. T. Fuhrman, H. Thoma, and N. P. Butch, Low-temperature crystal structure of the unconventional spin-triplet superconductor UTe_2 from single-crystal neutron diffraction, Acta Crystallogr., Sect. B **76**, 137 (2020).

[45] J. Gan, P. Coleman, and N. Andrei, Coexistence of Fermi Liquid and Magnetism in the Underscreened Kondo Problem, Phys. Rev. Lett. **68**, 3476 (1992).